

Synthesis, Crystal Structures, and Magnetic Properties of 2D Manganese(II) and 1D Gadolinium(III) Coordination Polymers with 1*H*-1,2,3-Triazole-4,5-dicarboxylic Acid

Wei Shi,^[a] Xiao-Yan Chen,^[a] Na Xu,^[a] Hai-Bin Song,^[b] Bin Zhao,^[a] Peng Cheng,^{*,[a]} Dai-Zheng Liao,^[a] and Shi-Ping Yan^[a]

Keywords: Manganese / Gadolinium / Coordination polymers / Magnetic properties / N,O ligands

Two new coordination polymers, namely $[\{\text{Mn}_3(\text{tda})_2(\text{H}_2\text{O})_6\} \cdot 6\text{H}_2\text{O}]_n$ (**1**) and $[\{\text{Gd}(\text{H}_2\text{O})_4(\text{Htda})\} \cdot (\text{H}_2\text{tda}) \cdot \text{H}_2\text{O}]_n$ (**2**) ($\text{H}_3\text{tda} = 1H$ -1,2,3-triazole-4,5-dicarboxylic acid), have been prepared and characterized by IR spectroscopy, elemental analysis, and single-crystal X-ray diffraction. Polymer **1** is a novel 2D stair-like coordination polymer, while **2** is a 1D

chain. Temperature-dependent magnetic measurements indicate the existence of antiferromagnetic interactions in both **1** and **2**.

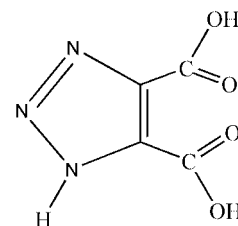
(© Wiley-VCH Verlag GmbH & Co. KGaA, 69451 Weinheim, Germany, 2006)

Introduction

The design and construction of architectures with appealing topologies have been attracting considerable attention in supramolecular chemistry and crystal engineering in recent years.^[1] Among them, the use of metal ions as nodes and bridging ligands as spacers has had a large impact on the building of coordination polymers with novel structures and is expected to lead to the development of exploitable properties such as magnetism, molecular sensors, luminescent materials, absorption materials, and so on.^[2] Although many intriguing complexes have been well documented as 1D chains^[3] and ladders,^[4] 2D grids,^[5] 3D frameworks, and helical staircase networks^[6] in previous studies, the rational design of specific complexes with the above-mentioned properties is still a challenge for chemists.

The selection of polydentate organic compounds as ligands is a key point in the design and assembly of the expected complexes. In our previous studies, pyridine-2,6-dicarboxylic acid, pyridine-2,5-dicarboxylic acid, pyridine-2,4,6-tricarboxylic acid, and related derivatives have been employed for the construction of novel structures with dimensionalities from discrete to 3D, and with useful properties such as luminescence.^[7] This type of ligand is based on the six-membered aromatic ring of pyridine with carboxylic groups in different sites as substituents. As a continuation of this work, we focus our attention here on the ligand

based on the five-membered heterocycle dicarboxylic derivative H_3tda ($\text{H}_3\text{tda} = 1H$ -1,2,3-triazole-4,5-dicarboxylic acid). The molecular structure of this ligand is shown in Scheme 1. Most studies of H_3tda with metal ions are in the solution state,^[8] and only two examples of rhodium(II) and copper(II) complexes with crystal structures of this ligand have been reported as far as we know.^[9]



Scheme 1.

In this contribution, two coordination polymers, namely $[\{\text{Mn}_3(\text{tda})_2(\text{H}_2\text{O})_6\} \cdot 6\text{H}_2\text{O}]_n$ (**1**) and $[\{\text{Gd}(\text{H}_2\text{O})_4(\text{Htda})\} \cdot (\text{H}_2\text{tda}) \cdot \text{H}_2\text{O}]_n$ (**2**), are reported. The metal ions manganese(II) and gadolinium(III) were used for magnetic studies for two reasons: (a) they possess the highest spin ground state in transition metal ions and lanthanide metal ions (${}^6\text{A}_{1g}$ for Mn^{II} and ${}^8\text{S}_{7/2}$ for Gd^{III}), and always show important magnetic behaviors; (b) the first-order orbital moment of these two metal ions is completely quenched by the ligand field so that the magnetic behavior can be effectively analyzed with the expression derived from the pure spin Hamiltonian. Both of the complexes were characterized by IR spectroscopy, elemental analysis, and single-crystal X-ray diffraction. Polymer **1** is a novel stair-like 2D network based on trinuclear isosceles triangular Mn_3 secondary building units, while **2** is a 1D coordination polymer. Tem-

[a] Department of Chemistry, Nankai University, Tianjin, 300071, P. R. China
Fax: +86-22-2350-2458
E-mail: pcheng@nankai.edu.cn

[b] State Key Laboratory of Elemento-Organic Chemistry, Nankai University, Tianjin 300071, P. R. China

perature-dependent magnetic measurements show that there are antiferromagnetic interactions in both **1** and **2**.

Results and Discussion

Description of the Structure

$[\{ \text{Mn}_3(\text{tda})_2(\text{H}_2\text{O})_6 \} \cdot 6\text{H}_2\text{O}]_n$ (**1**)

Polymer **1** crystallizes in the orthorhombic space group *Pmna* with two crystallographically independent Mn^{II} ions in the crystal lattice, as shown in Figure 1. Mn1 lies in a

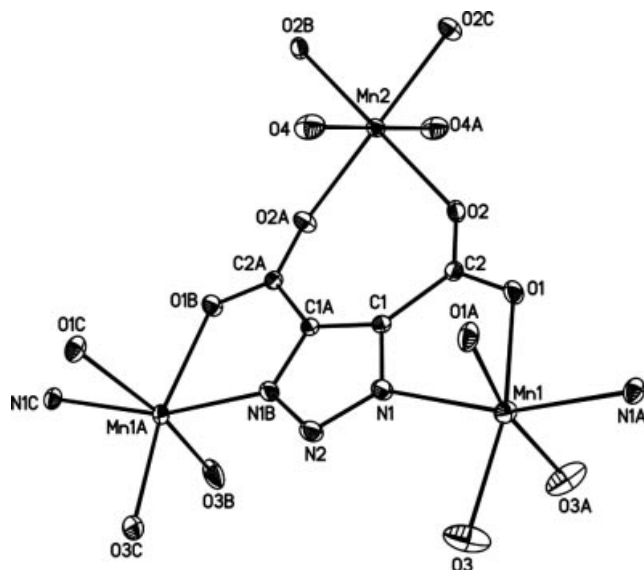


Figure 1. The molecular unit of **1**. Hydrogen bonds and lattice water molecules have been omitted for clarity.

distorted octahedral environment. The equatorial plane contains O1 and O1A [Mn1–O1(O1A) 2.219(2) Å] from the carboxylate groups and O3 and O3A [Mn1–O3(O3A) 2.139(3) Å] from coordinated water molecules. N1 and N1A [Mn1–N1 2.240(3) Å] from the tda^{3-} ligand occupy the axial direction with an N1–Mn1–N1A angle of 162.22(14)°. Mn2 lies in a centrosymmetrical octahedral environment, which is completed by O2, O2A, O2B, and O2C [Mn2–O2 2.158(2) Å] from the carboxylate groups in the equatorial plane and O4 and O4A [Mn2–O4 2.190(4) Å] from the coordinated water molecules in the axial positions. O2, O2A, O2B, and O2C are perfectly coplanar, and O4, Mn2, and O4A are completely co-linear. The tda^{3-} ligand exhibits an unusual hexadentate binding mode, chelating three Mn^{II} ions. It should be noted that all the atoms of every tda^{3-} ligand are essentially coplanar. The maximum deviation from the plane containing N1, N2, and N1A is 0.07 Å, with an average value of 0.00 Å. This suggests that a conjugated π_{11}^{14} bond delocalized over both the triazole ring and the carboxylate groups may exist in the structure. The Mn1...Mn1A and Mn1...Mn2 distances are 6.579(6) and 6.190(5) Å, respectively. As shown in Figure 2 (a), every tda^{3-} ligand further bridges two crystallographically identical Mn1 ions to form a 1D chain in the *a* direction. Furthermore, these chains are linked through the Mn2 ions coordinated to the carboxylate groups of tda^{3-} in the *c* direction to form a 1D ladder-like structure comprising Mn6 coordination rings. Importantly, the molecular planes of the tda^{3-} anions in the 1D chain are perpendicular to each other, and the 1D ladders are further assembled into a novel 2D stair-like network in which the plane of every ladder is also perpendicular (Figure 2, b). This particular supramolecular structure is rather rare among known molecular

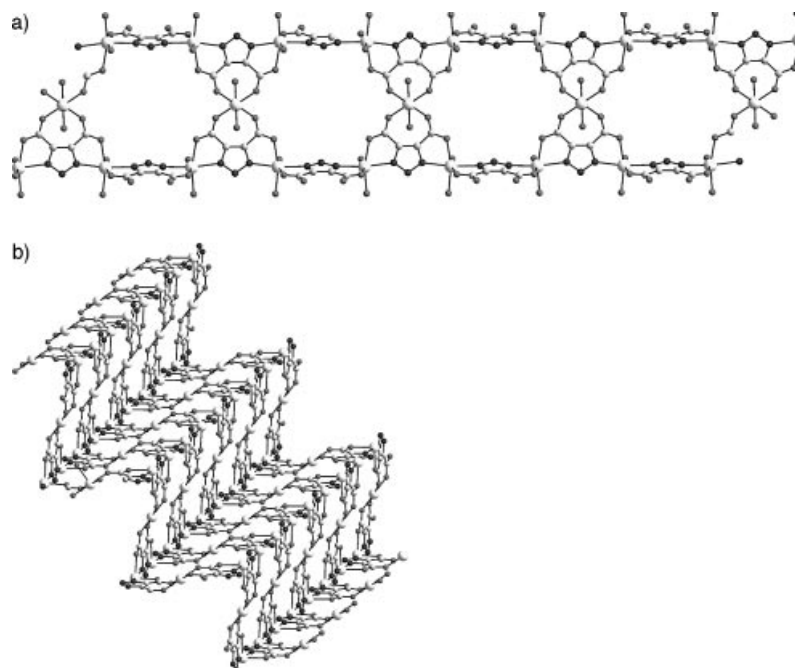


Figure 2. (a) The ladder like structure of **1** viewed along the *a* axis. (b) The 2D stair-like structure of **1**. Water molecules coordinated to the Mn^{II} ions have been omitted for clarity.

frameworks.^[10] In the crystal, the 2D networks are connected by hydrogen bonds to form a 3D supramolecular architecture containing 1D channels along the *b* direction, as shown in Figure 3.

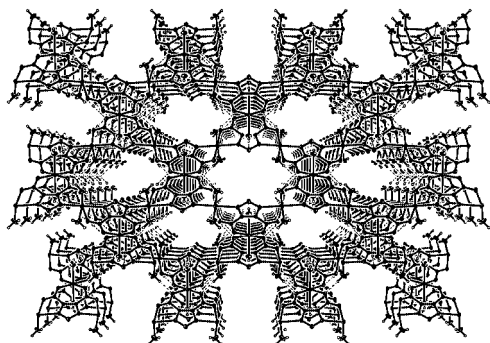
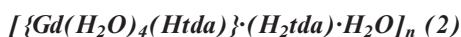


Figure 3. The 3D supramolecular architecture of **1** viewed down the *b* axis. Lattice water molecules in the channel have been omitted for clarity.



Polymer **2** crystallizes in the monoclinic space group *C2/c*. There is only one crystallographically independent

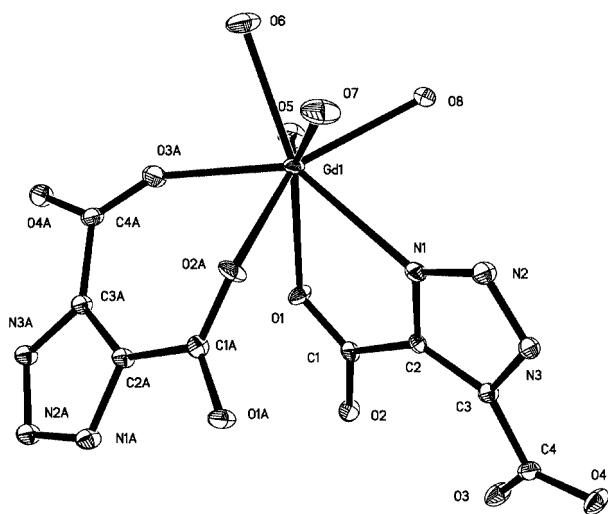


Figure 4. Diagram showing the coordination environment of the Gd^{III} ion in **2**. Hydrogen atoms have been omitted for clarity.

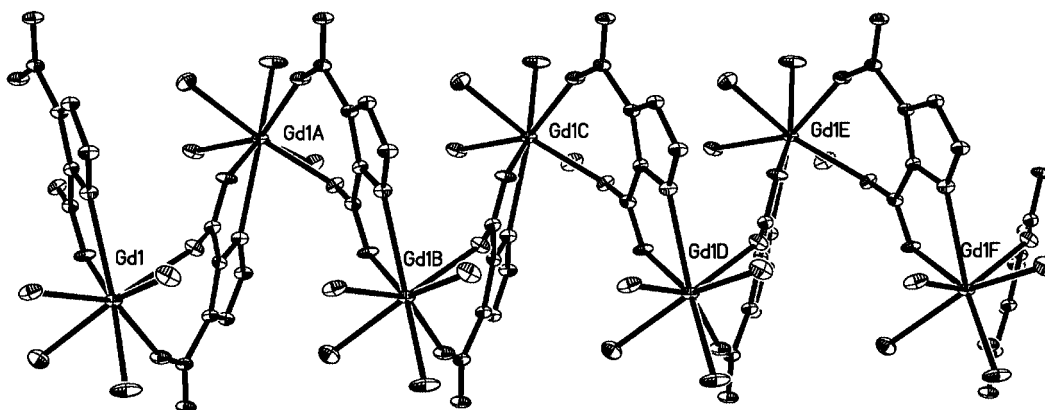


Figure 5. Diagram showing the 1D zigzag chain of **2**. Hydrogen atoms have been omitted for clarity.

Gd^{III} ion in the crystal lattice. As shown in Figure 4 this Gd^{III} ion is eight-coordinate, with three oxygen atoms and one nitrogen atom from the Htda^{2-} ligand and four water molecules, which together form a square-antiprismatic coordination environment. The $\text{Gd}-\text{N}$ bond length is 2.582(5) Å, and that of $\text{Gd}-\text{O}$ is in the range 2.318(4)–2.437(4) Å, with an average value of 2.379(4) Å. Every Htda^{2-} ligand links two Gd^{III} ions to form a 1D zigzag chain in the *b* direction, as shown in Figure 5. Moreover, the 1D zigzag chains are linked by intermolecular hydrogen bonds between the nitrogen atoms in the triazole ring and the oxygen atoms of the carboxylate groups to form 2D layers. These layers are further linked through the counterions of H_2tda^- and lattice water molecules into a 3D supramolecular network, as shown in Figure 6.

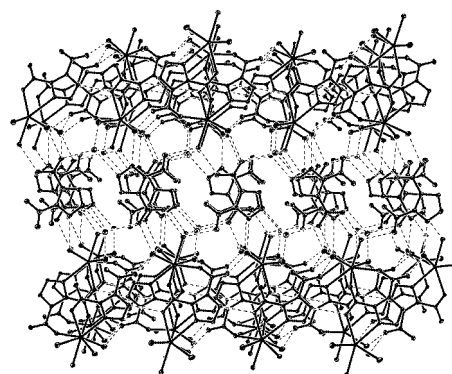
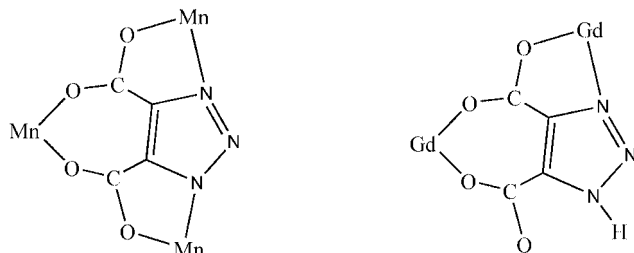


Figure 6. The 3D supramolecular architecture of **2** linked through the counterions of Htda^- . Dotted lines represent hydrogen bonding interactions.

The coordination modes of **1** and **2** are shown in Scheme 2. The proton in the 1-position in the triazole ring plays an important role in the formation of the two different coordination modes. For charge neutralization, it is suggested that the ligand is completely deprotonated, existing as tda^{3-} in **1**. The nitrogen atoms in the 1- and 3-positions in the triazole ring become identical from a chemical viewpoint and the tda^{3-} ligand therefore has C_2 symmetry. In **2**, the ligand is only doubly deprotonated (at the carboxylate groups) therefore it exists as Htda^{2-} and only has C_1 sym-

metry. The different symmetries of the ligands result in different coordination modes.



Scheme 2.

Infrared Spectra

The main features in the IR spectra of both **1** and **2** mainly concern the carboxylate groups and the triazole rings. In **1**, a very strong band appears at around 1595 cm^{-1} due to the antisymmetric stretching (ν_{as}) of the carboxylate group; the symmetrical stretching (ν_{s}) band of this group appears at 1470 and 1445 cm^{-1} , respectively. The difference between ν_{as} and ν_{s} is lower than 200 cm^{-1} , which indicates the $\mu_{1,3}$ -bridging mode of the carboxylate group to the metal ion, in agreement with the X-ray crystal analysis.^[11] In **2**, the ν_{as} and ν_{s} absorptions appear at 1631 and 1380 cm^{-1} , respectively. The bands at 1499 , 1464 , 1016 , and 781 cm^{-1} may be attributed to the $\nu(\text{C}-\text{N})$ stretching of the triazole ring.

Magnetic Properties

In order to understand the magnetic interactions between the paramagnetic ions via the H_3tda ligand in such 1D and 2D structures, the magnetic susceptibilities (χ_{M}) of both compounds were measured on a Quantum Design MPMS-5S SQUID magnetometer in a field of 1000 Oe. The plots of χ_{M} and μ_{eff} vs. T are shown in Figures 7 and 8 for **1** and **2**, respectively. For **1**, the magnetic susceptibilities were measured in the temperature range from 2 to 300 K. The room-temperature value of $10.23\text{ }\mu_{\text{B}}$ for μ_{eff} is close to the value of $10.25\text{ }\mu_{\text{B}}$, which is the spin-only value expected for three free Mn^{II} ions with isotropic $g = 2.00$. As the temperature decreases, the value of μ_{eff} decreases smoothly, and below 50 K it decreases abruptly to a minimum of $3.52\text{ }\mu_{\text{B}}$ at 2 K. This curve is in agreement with an antiferromagnetic coupling between the Mn^{II} ions. An analytical expression of magnetic susceptibilities for this kind of 2D Mn^{II} complex is not available and only an approximate approach based on both the structural and magnetic data can be performed.^[12] Here, we first use the Curie–Weiss law to analyze the experimental data. The best fit gives a Curie constant, C , of $4.57\text{ emu K mol}^{-1}$ and a Weiss constant, θ ,

of -15.47 K , which is consistent with the μ_{eff} vs. T curve for the antiferromagnetic interactions in **1**. Secondly, based on the crystal data, there are two main pathways ($\text{Mn}-\text{O}-\text{C}-\text{O}-\text{Mn}$ and $\text{Mn}-\text{N}-\text{N}-\text{N}-\text{Mn}$) to transfer the magnetic interactions. By considering that the isosceles triangular Mn_3 unit is the basic building block, the expression derived from the Hamiltonian $H = -2J_1S_2(S_1 + S_3) - 2J_2S_1S_3$ (where J_1 is the coupling constant between $\text{Mn}1$ and $\text{Mn}2$, and J_2 is the coupling constant between $\text{Mn}1$ and $\text{Mn}1\text{A}$; see Figure 1 and Scheme 3) was used to fit the data.^[13] Because the trinuclear units further assemble into a 2D structure, a θ parameter was considered to correct the possible secondary effects such as the interactions between the Mn_3 units and/or the zero-field splitting of the Mn^{II} ion.^[13] The least-squares fit gives $J_1 = -17.99\text{ cm}^{-1}$, $J_2 = -9.3\text{ cm}^{-1}$, $\theta = -3.9\text{ K}$, and $g = 2.00$, with an agreement factor, R , of 9.54×10^{-4} ($R = \sum(\chi_{\text{obsd}} - \chi_{\text{calcd}})^2 / \sum(\chi_{\text{obsd}}^2)$). The J_1 value of **1** is obviously larger than other single carboxylato-bridged Mn^{II} complexes, such as $[\{\text{Mn}(\text{bipy})_2(\text{H}_2\text{O})\}_2\{(\text{CH}_3)_3\text{NCH}_2\text{CO}_2\}](\text{ClO}_4)_4 \cdot 2\text{H}_2\text{O}$ ($g = 1.97$, $J = -0.193\text{ cm}^{-1}$) and $[\text{Mn}(\text{MCPA})_2(\text{H}_2\text{O})_2]_n$ (MCPA = 2-methyl-4-chlorophenoxyacetic acid; $g = 1.90$, $J = -0.30\text{ cm}^{-1}$).^[14] The reason for this may be that the delocalized electrons not only appear around the carboxylate groups but also reside on the tda^{3-}

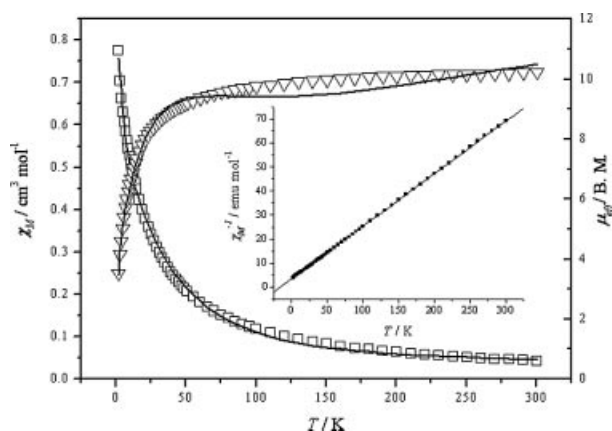


Figure 7. Plots of χ_{M} (\square) and μ_{eff} (∇) vs. the temperature for **1**; the solid line represents the best fit. Inset: the Curie–Weiss fit.

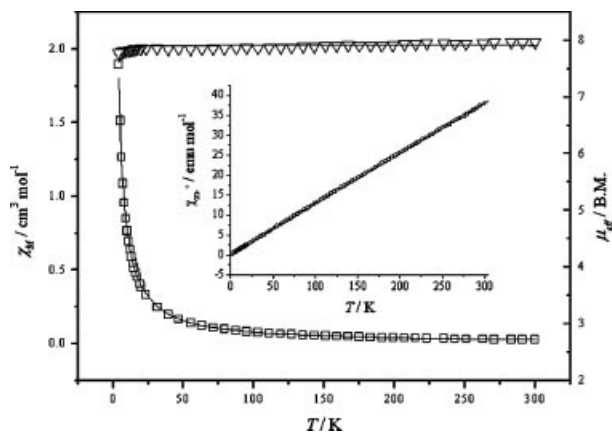
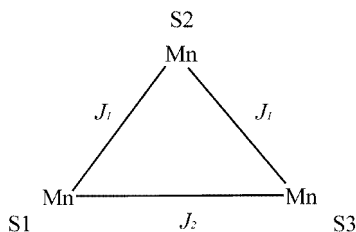


Figure 8. Plots of χ_{M} (\square) and μ_{eff} (∇) vs. the temperature for **2**; the solid line represents the best fit.

anion, which enhances the capability for magnetic exchange. By comparing the J_1 and J_2 values, the ability of triazole for magnetic exchange is seen to be smaller than that of the carboxylate group. These results indicate that the tda^{3-} anion is a favorable bridging ligand for magnetic exchange of paramagnetic metal ions.



Scheme 3.

Since the Gd^{III} ion in **2** lies in the $^8S_{7/2}$ singlet ground state and does not possess a first-order orbital moment, its magnetic properties are amenable to a rather simple analysis based on a spin-only Hamiltonian. The μ_{eff} value of **2** at room temperature is $7.97 \mu_{\text{B}}$, which compares well with the theoretical value of $7.94 \mu_{\text{B}}$ for one isolated Gd^{III} ion with an isotropic g value of 2.00. The μ_{eff} value remains almost constant with a decrease of temperature to 2 K, which indicates that the interactions transferred through the H_3tda ligand are very weak. The Curie–Weiss fit for the experimental data gives a Curie constant of $7.89 \text{ emu K mol}^{-1}$ and a Weiss constant of -0.85 K . The theoretical χ_{m} is given by the following expression, which is based on the spin Hamiltonian $H = -J\sum_i S_i S_{i+1}$ with the quantum numbers $S_{\text{Gd}} = 7/2$:^[15]

$$\chi_{\text{M}} = \frac{N\beta^2 g^2 S(S+1)}{3kT} \cdot \frac{1+u}{1-u}$$

$$u = \coth\left[\frac{JS(S+1)}{kT}\right] - \left[\frac{kT}{JS(S+1)}\right]$$

Least-squares fitting of the experimental data leads to $J = -0.10 \text{ cm}^{-1}$, $g = 2.00$, and an agreement factor, R , of 6.9×10^{-4} . These results indicate a very weak antiferromagnetic interaction between the Gd^{III} ions. The magnitude of J is small but is of the same order as other Gd^{III} complexes.^[16] The reason for this may be that the 4f electrons lie closer to the metal center than the 5d and 6s electrons and are less influenced by the surrounding environment.

A qualitative interpretation of the magnetic interactions in such metal ions with half-filled orbitals can be made by the well-known Kahn model. The exchange integral (J) can be decomposed into two terms, one involving ferromagnetic (J_{F}) and the other antiferromagnetic contributions (J_{AF}).^[17] The value of J_{AF} is proportional to the square of the integral overlap and is always much larger in magnitude than J_{F} . Since the orbitals of Mn^{II} and Gd^{III} ions are both half-filled such that the electron cloud is completely symmetrical, the nonzero overlap integral of the magnetic orbitals of Gd^{III} or Mn^{II} would result in an antiferromagnetic interaction.

EPR Spectra

The manganese(II) ion has an $S = 5/2$ electronic spin, and ^{55}Mn has a high natural abundance of 100% and an $I = 5/2$ nuclear spin. The X-band EPR spectra of **1** in both the solid state and dmsO solution were recorded at room temperature. Only broad bands centered at $g \approx 2.00$ were observed, and no hyperfine pattern could be resolved. This may be due to the strong antiferromagnetic between manganese(II) ions and/or the resonance from the zero-field splitting.^[13]

Theoretical Investigation of tda^{3-}

As mentioned in the crystal structure discussion, a conjugated π_{11}^4 bond may exist in the tda^{3-} anion as all its atoms are almost coplanar. A charge density distribution calculation was performed on tda^{3-} at the DFT/B3LYP/6-311G* level using the Gaussian 98 program.^[18] The atomic coordinates for input were taken from the crystal data. The calculation result shows that the three negative charges are almost averagely delocalized over the whole tda^{3-} anion, which indicates the existence of a conjugated π_{11}^4 bond.

Conclusions

We have synthesized two new coordination polymers with 1*H*-1,2,3-triazole-4,5-dicarboxylic acid. The results show that **1** is a novel 2D stair-like coordination polymer based on trinuclear isosceles triangular Mn_3 secondary building units, while **2** exists as a 1D chain. Although temperature-dependent magnetic measurements indicate only antiferromagnetic interactions in both **1** and **2**, the interesting structures with variable coordination modes of H_3tda indicate that further studies of this ligand should be made, especially for the construction of 3d–4f complexes.

Experimental Section

General Remarks: All reagents and solvents employed were commercially available and used as received without further purification. H_3tda was synthesized according to the literature method.^[19]

Synthesis of $[\{\text{Mn}_3(\text{tda})_2(\text{H}_2\text{O})_6\} \cdot 6\text{H}_2\text{O}]_n$ (1**):** A mixture of $\text{Mn}(\text{ClO}_4)_2 \cdot 6\text{H}_2\text{O}$ (0.145 g, 0.40 mmol), H_3tda (0.156 g, 1.0 mmol), and H_2O (8 mL) was put in a 20-mL acid digestion bomb and heated at 150°C for three days. The colorless crystals obtained were collected after washing with water ($2 \times 5 \text{ mL}$) in a yield of 52% (92 mg). $\text{C}_8\text{H}_{24}\text{Mn}_3\text{N}_6\text{O}_{20}$ (689.15): calcd. C 13.94, H 3.51, N 12.19; found C 14.31, H 3.77, N 12.55.

Synthesis of $[\{\text{Gd}(\text{H}_2\text{O})_4(\text{Htda})\} \cdot (\text{H}_2\text{tda}) \cdot \text{H}_2\text{O}]_n$ (2**):** A mixture of $\text{Mn}(\text{ClO}_4)_2 \cdot 6\text{H}_2\text{O}$ (0.091 g, 0.25 mmol), H_3tda (0.039 g, 0.25 mmol), $\text{Gd}(\text{ClO}_4)_3 \cdot 6\text{H}_2\text{O}$ (0.282 g, 0.25 mmol), and H_2O (15 mL) was refluxed in a 100-mL round-bottomed flask for 2 h. The precipitate was filtered off and the filtrate was left to stand at room temperature. Slow concentration of the resulting solution under ambient conditions led to the formation of colorless single crystals of **2** as the only solid with a yield of 86% (68 mg). Without the admixture of $\text{Mn}(\text{ClO}_4)_2 \cdot 6\text{H}_2\text{O}$ under the same conditions only

Table 1. Crystal data and structure refinement for **1** and **2**.

	1	2
Empirical formula	C ₈ H ₂₄ N ₆ O ₂₀ Mn ₃	C ₈ H ₁₃ N ₆ O ₁₃ Gd
<i>M_r</i>	689.15	558.49
Temperature [K]	293(2)	294(2)
Crystal system	orthorhombic	monoclinic
Space group	<i>Pmna</i>	<i>C2/c</i>
<i>a</i> [Å]	13.158(4)	35.000(10)
<i>b</i> [Å]	7.446(2)	6.860(2)
<i>c</i> [Å]	12.255(4)	14.179(4)
<i>α</i> [°]	90	90
<i>β</i> [°]	90	98.183(5)
<i>γ</i> [°]	90	90
<i>V</i> [Å ³]	1200.6(6)	3369.4(17)
<i>Z</i>	2	8
<i>D</i> _{calcd.} [mg m ^{−3}]	1.906	2.202
<i>μ</i> [mm ^{−1}]	1.655	4.022
<i>θ</i> [°]	2.27–25.00	1.18–26.57
Index ranges	−15 ≤ <i>h</i> ≤ 15 −8 ≤ <i>k</i> ≤ 8 −14 ≤ <i>l</i> ≤ 9	−33 ≤ <i>h</i> ≤ 44 −8 ≤ <i>k</i> ≤ 8 −17 ≤ <i>l</i> ≤ 17
Reflections collected	5795	8853
Independent reflections	1112, <i>R</i> (int) = 0.0445	3497, [<i>R</i> (int) = 0.0470]
Max, min transmission	1.000000 and 0.749560	1.000000 and 0.525940
Data/restraints/parameters	1112/9/97	3497/5/262
Goodness-of-fit on <i>F</i> ²	1.076	1.052
<i>R</i> ₁ , <i>wR</i> ₂ [<i>I</i> > 2σ (<i>I</i>)]	0.0354, 0.0850	0.0420, 0.1052
<i>R</i> ₁ , <i>wR</i> ₂ (all data)	0.0501, 0.0920	0.0549, 0.1116
Largest diff. peak and hole [e Å ^{−3}]	0.413 and −0.485	2.209 and −2.211

a powder sample of **2** was obtained, as confirmed by IR spectroscopy, elemental analyses, and PXRD. C₈H₁₃GdN₆O₁₃ (545.48): calcd. C 17.21, H 2.35, N 15.05; found C 16.85, H 2.42, N 15.19.

Physical Techniques: C, H, and N analyses were obtained at the Institute of Elemental Organic Chemistry, Nankai University. The FT-IR spectra were measured with a Bruker Tensor 27 Spectrom-

eter on KBr disks. Variable-temperature magnetic susceptibilities were measured on a Quantum Design MPMS-5S SQUID magnetometer. Diamagnetic corrections were made with Pascal's constants for all the constituent atoms.

X-ray Crystallographic Studies: The structural determinations of **1** and **2** were performed by single-crystal XRD analyses. Determinations of the unit cell and data collection were performed with Mo-*K*_α radiation (*λ* = 0.71073 Å) on a Bruker Smart 1000 diffractometer equipped with a CCD camera. The ω-φ scan technique was employed. Crystal parameters and structure refinements for **1** and **2** are summarized in Table 1. Selected bond lengths and angles are listed in Table 2.

The structures were solved primarily by direct methods and Fourier difference techniques and refined by the full-matrix least-squares method. The computations were performed with the SHELXL-97 program.^[20] All non-hydrogen atoms were refined anisotropically. The hydrogen atoms were set in calculated positions and refined as riding atoms with a common fixed isotropic thermal parameter.

CCDC-290628 (for **1**) and -287164 (for **2**) contain the supplementary crystallographic data for this paper. These data can be obtained free of charge from The Cambridge Crystallographic Data Centre via www.ccdc.cam.ac.uk/data_request/cif.

Acknowledgments

This work was supported by the National Natural Science Foundation of China (grant nos. 90501002 and 20425103), the NSF of Tianjin (grant no. 06YFJZJC009000), and the State Key Project of Fundamental Research of MOST (2005CCA01200), P. R. China.

Table 2. Selected bond lengths [Å] and angles [°] for **1** and **2**.

1 ^[a]			
Mn1–O3	2.139(3)	Mn1–N1	2.240(3)
Mn1–O1	2.219(2)	Mn2–O2	2.158(2)
Mn2–O4	2.190(4)		
O3A–Mn1–O3	88.57(17)	O2A–Mn2–O2	91.35(12)
O3A–Mn1–O1	91.87(11)	O1–Mn1–O1A	90.87(14)
O3–Mn1–O1	166.39(10)	O3–Mn1–N1A	98.49(11)
O1–Mn1–N1	72.26(9)	O1–Mn1–N1A	95.04(9)
O1A–Mn1–N1	95.04(9)	O3A–Mn1–N1	98.49(11)
N1A–Mn1–N1	162.22(14)	O2–Mn2–O4A	92.96(9)
O2C–Mn2–O2B	88.65(12)		
2 ^[b]			
Gd1–O3A	2.318(4)	Gd1–O8	2.394(4)
Gd1–O7	2.347(5)	Gd1–O5	2.420(4)
Gd1–O2A	2.365(4)	Gd1–O1	2.437(4)
Gd1–O6	2.372(5)	Gd1–N1	2.582(5)
O7–Gd1–O6	74.75(18)	O8–Gd1–O1	106.43(16)
O7–Gd1–O8	82.06(18)	O5–Gd1–O1	73.33(16)
O6–Gd1–O8	81.82(18)	O7–Gd1–N1	80.27(18)
O7–Gd1–O5	146.87(17)	O6–Gd1–N1	146.51(16)
O6–Gd1–O5	78.22(18)	O8–Gd1–N1	72.86(16)
O8–Gd1–O5	75.42(17)	O5–Gd1–N1	114.82(17)
O7–Gd1–O1	137.39(16)	O1–Gd1–N1	63.73(14)
O6–Gd1–O1	146.95(15)		

[a] A: $-x + 1/2$, y , $-z + 1/2$; B: x , $-y + 1$, $-z$; C: $-x + 1$, $-y + 1$, $-z$. [b] A: $-x + 1/2$, $y + 1/2$, $-z + 1/2$.

- Lo, J. P. H. Charmant, A. G. Orpen, I. D. Williams, *Science* **1999**, 283, 1148–1150; d) H. Li, M. Eddaoudi, M. O’Keeffe, O. M. Yaghi, *Nature* **1999**, 402, 276–279; e) M. Albrecht, M. Luta, A. L. Spek, G. van Koten, *Nature* **2000**, 406, 970–974; f) R. Owen, W. Lin, *Acc. Chem. Res.* **2002**, 35, 511–522.
- [2] a) D. W. Bruce, D. O’Hare *Inorganic Materials*, Wiley, Chichester, UK, **1992**; b) O. Kahn, *Molecular Magnetism*, VCH, New York, **1993**; c) E. Holder, B. M. W. Langeveld, U. S. Schubert, *Adv. Mater.* **2005**, 17, 1109–1121; d) J. C. G. Bunzli, G. R. Choppin, *Lanthanide Probes in Life, Chemical and Earth Sciences*, Elsevier, New York, **1989**; e) B. Valeur, *Molecular Fluorescence: Principles and Applications*, Wiley-VCH, **2001**; f) M. Eddaoudi, D. B. Moler, H. L. Li, B. L. Chen, T. M. Reineke, M. O’Keeffe, O. M. Yaghi, *Acc. Chem. Res.* **2001**, 34, 319–330.
- [3] a) D. M. Shin, I. S. Lee, Y. A. Lee, Y. K. Chung, *Inorg. Chem.* **2003**, 42, 2977–2982; b) M. A. Withersby, A. J. Blake, N. R. Champness, P. Hubberstey, W. S. Li, M. Schröder, *Angew. Chem. Int. Ed. Engl.* **1997**, 36, 2327–2329; c) A. S. Batsanov, M. J. Begley, P. Hubberstey, J. Stroud, *J. Chem. Soc., Dalton Trans.* **1996**, 1947–1957.
- [4] a) M. A. Withersby, A. J. Blake, N. R. Champness, P. A. Cooke, P. Hubberstey, W. S. Li, M. Schröder, *Inorg. Chem.* **1999**, 38, 2259–2266; b) K. Nomiyama, H. Yokoyama, *J. Chem. Soc., Dalton Trans.* **2002**, 2483–2490.
- [5] a) D. M. Shin, I. S. Lee, Y. K. Chung, M. S. Lah, *Inorg. Chem.* **2003**, 42, 5459–5461; b) K. Mitsurs, M. Shimamura, S. I. Noro, S. Minakoshi, A. Asami, K. Seki, S. Kitagawa, *Chem. Mater.* **2000**, 12, 1288–1299; c) L. Carlucci, G. Ciani, D. M. Proserpio, *J. Chem. Soc., Dalton Trans.* **1999**, 1799–1804; d) C. He, B. G. Zhang, C. Y. Duan, J. H. Li, Q. J. Meng, *Eur. J. Inorg. Chem.* **2000**, 2549–2554.
- [6] a) M. Eddaoudi, J. Kim, N. Rosi, D. Vodak, J. Wachter, M. O’Keeffe, O. M. Yaghi, *Science* **2002**, 295, 469–472; b) C. D. Wu, C. Z. Lu, H. H. Zhuang, J. S. Huang, *J. Am. Chem. Soc.* **2002**, 124, 3836–3837; c) T. M. Reineke, M. Eddaoudi, D. Moler, M. O’Keeffe, O. M. Yaghi, *J. Am. Chem. Soc.* **2000**, 122, 4843–4844; d) R. B. Stuart, R. Richard, *Angew. Chem. Int. Ed.* **1998**, 37, 1460–1494.
- [7] a) B. Zhao, P. Cheng, Y. Dai, C. Cheng, D. Z. Liao, S. P. Yan, Z. H. Jiang, G. L. Wang, *Angew. Chem. Int. Ed.* **2003**, 42, 934–936; b) B. Zhao, P. Cheng, X. Y. Chen, C. Cheng, W. Shi, D. Z. Liao, S. P. Yan, Z. H. Jiang, *J. Am. Chem. Soc.* **2004**, 126, 3012–3013; c) B. Zhao, X. Y. Chen, P. Cheng, D. Z. Liao, S. P. Yan, Z. H. Jiang, *J. Am. Chem. Soc.* **2004**, 126, 15394–15395; d) B. Zhao, H. L. Gao, X. Y. Chen, P. Cheng, W. Shi, D. Z. Liao, S. P. Yan, Z. H. Jiang, *Chem. Eur. J.* **2006**, 12, 149–158; e) H. L. Gao, C. Cheng, B. Ding, W. Shi, H. B. Song, P. Cheng, D. Z. Liao, S. P. Yan, Z. H. Jiang, *J. Mol. Struct.* **2005**, 738, 105–111; f) H. L. Gao, L. Yi, B. Ding, H. S. Wang, P. Cheng, D. Z. Liao, S. P. Yan, *Inorg. Chem.* **2006**, 45, 481–483.
- [8] a) L. D. Hansen, B. D. West, E. J. Baca, C. L. Blank, *J. Am. Chem. Soc.* **1968**, 90, 6588–6592; b) A. D. Robertis, C. Foti, A. Gianguzza, *J. Chem. Res. S* **1995**, 7, 288–289; c) F. Capitan, F. Salinas, E. J. Alonso, *Anal. Quim.* **1973**, 69, 1133–1139; d) F. Capitan, F. Salinas, E. J. Alonso, *Bol. Soc. Quim. Peru* **1973**, 39, 1–14.
- [9] a) C. Net, J. C. Bayon, P. Esteban, *Inorg. Chem.* **1993**, 32, 5313–5321; b) J. R. Olson, M. Yamauchi, *Inorg. Chim. Acta* **1985**, 99, 121–128.
- [10] L. Zhang, P. Cheng, L. F. Tang, L. H. Weng, Z. H. Jiang, D. Z. Liao, S. P. Yan, G. L. Wang, *Chem. Commun.* **2000**, 717–718.
- [11] K. Nakamoto, *Infrared and Raman Spectra of Inorganic and Coordination Compounds*, 4th ed., Wiley Press, **1986**.
- [12] a) E. Q. Gao, Y. F. Yue, S. Q. Bai, Z. He, S. W. Zhang, C. H. Yan, *Chem. Mater.* **2004**, 16, 1590–1596; b) B. Bitschnau, A. Egger, A. Escuer, F. A. Mautner, B. Sodin, R. Vicente, *Inorg. Chem.* **2006**, 45, 868–876.
- [13] R. L. Carlin, *Magnetochemistry*, Springer-Verlag, Berlin, **1986**.
- [14] a) X. M. Chen, Y. X. Tong, Z. T. Xu, T. C. W. Mak, *J. Chem. Soc., Dalton Trans.* **1995**, 4001–4004; b) V. Tangoulis, G. Psomas, C. Dendrinou-Samara, C. P. Raptopoulou, A. Terzis, D. P. Kessissoglou, *Inorg. Chem.* **1996**, 35, 7655–7660.
- [15] M. E. Fisher, *Am. J. Phys.* **1964**, 32, 343–346.
- [16] M. Hernandez-Molina, C. Ruiz-Perez, T. Lopez, F. Lloret, M. Julve, *Inorg. Chem.* **2003**, 42, 5456–5458.
- [17] O. Kahn, M. F. Charlot, *Nouv. J. Chim.* **1980**, 4, 567–576.
- [18] M. J. Frisch, G. W. Trucks, H. B. Schlegel, G. E. Scuseria, M. A. Robb, J. R. Cheeseman, V. G. Zakrzewski, J. A. Montgomery, Jr., R. E. Stratmann, J. C. Burant, S. Dapprich, J. M. Millam, A. D. Daniels, K. N. Kudin, M. C. Strain, O. Farkas, J. Tomasi, V. Barone, M. Cossi, R. Cammi, B. Mennucci, C. Pomelli, C. Adamo, S. Clifford, J. Ochterski, G. A. Petersson, P. Y. Ayala, Q. Cui, K. Morokuma, D. K. Malick, A. D. Rabuck, K. Raghavachari, J. B. Foresman, J. Cioslowski, J. V. Ortiz, A. G. Baboul, B. B. Stefanov, G. Liu, A. Liashenko, P. Piskorz, I. Komaromi, R. Gomperts, R. L. Martin, D. J. Fox, T. Keith, M. A. Al-Laham, C. Y. Peng, A. Nanayakkara, M. Challacombe, P. M. W. Gill, B. Johnson, W. Chen, M. W. Wong, J. L. Andres, C. Gonzalez, M. Head-Gordon, E. S. Replogle, J. A. Pople, *Gaussian 98, Revision A.9*, Gaussian, Inc., Pittsburgh PA, **1998**.
- [19] L. E. Hinkel, G. O. Richards, O. Thomas, *J. Chem. Soc.* **1937**, 1432–1437.
- [20] a) G. M. Sheldrick, *SHELXS 97, Program for the Solution of Crystal Structures*, University of Göttingen, Germany, **1997**; b) G. M. Sheldrick, *SHELXL 97, Program for the Refinement of Crystal Structures*, University of Göttingen, Germany, **1997**.

Received: July 4, 2006

Published online: October 2, 2006